Application of the gradient method to Hartree-Fock-Bogoliubov theory

L. M. Robledo and G. F. Bertsch

Phys. Rev. C **84**, 014312 — Published 13 July 2011

DOI: 10.1103/PhysRevC.84.014312

Application of the gradient method to Hartree-Fock-Bogoliubov theory

L.M. Robledo[1] and G.F. Bertsch[2]

[1]*Departamento de Fisica Teorica, Univeridad Autonoma de Madrid, E-28049 Madrid, Spain*

[2]*Institute for Nuclear Theory and Dept. of Physics,*

University of Washington, Seattle, Washington

Abstract

A computer code is presented for solving the equations of Hartree-Fock-Bogoliubov (HFB) theory by the gradient method, motivated by the need for efficient and robust codes to calculate the configurations required by extensions of HFB such as the generator coordinate method. The code is organized with a separation between the parts that are specific to the details of the Hamiltonian and the parts that are generic to the gradient method. This permits total flexibility in choosing the symmetries to be imposed on the HFB solutions. The code solves for both even and odd particle number ground states, the choice determined by the input data stream. Application is made to the nuclei in the *sd*-shell using the USDB shell-model Hamiltonian.

I. INTRODUCTION

An important goal of nuclear structure theory is to develop the computational tools for a systematic description of nuclei across the chart of the nuclides. There is hardly any alternative to self-consistent mean-field (SCMF) for the starting point of a global theory, but the SCMF has to be extended by the generator coordinate method (GCM) or other means to calculate spectroscopic observables. There is a need for computational tools to carry out the SCMF efficiently in the presence of the multiple constraints to be used for the GCM. Besides particle number, quantities that may be constrained include moments of the density, angular momentum, and in the Hartree-Fock-Bogoliubov (HFB) theory, characteristics of the anomalous densities. Because the HFB theory includes correlations that are important in heavy nuclei, it is the preferred based starting point for GCM and other extensions.

Like Hartree-Fock, the HFB is founded on a variational principle for the energy of the system. In the case of Hartree-Fock, the many-body wave function is varied in the space of Slater determinants. In the HFB theory, the variation is in the more general space defined by the Bogoliubov transformation. Both theories can be concisely formulated for Hamiltonians that are expressible in second quantized notation. For ordinary two-body Hamiltonians, the energy to be minimized $\langle \hat{H} \rangle$ is given by Eq. (3) below, or more generally Eq. (18) in the presence of constraints. As a nonlinear minimization problem, there are no efficient algorithms that apply to all cases. In the nuclear HFB as well as Hartree-Fock problem, it is very common practice replace the minimization problem by the problem of finding zeros of a function of many variables, formally $\delta\langle \hat{H} \rangle / \delta\phi_i = 0$ where ϕ_i is a wave function amplitude. This yields the HFB matrix eigenvalue equation, for which there are many codes available in the literature, eg. [4–8]. However, as will be discussed below, the matrix eigenvalue method can have problems particularly when there are many constraints on the solution. In contrast, the gradient method described by Ring and Schuck ([1], Section 7.3.3) is quite robust and easily deals with multiple constraints. However, the computational aspects of the method as applied to HFB have not been well documented in the literature in the detail that is found for example in Ref. [2], describing the corresponding algorithm for nuclear Hartree-Fock theory. And we know of no published codes applicable to the nuclear problem.

Here we will describe an implementation of the gradient algorithm for HFB following the iterative method used by Robledo and collaborators [10]. The main aspects of that

method up to Eq. (22) below has also been described in Ref. [9]. The code presented here, `hfb_shell`, is available as supplementary material to this article (see Appendix). The code has separated out the parts that are basic to the gradient method and the parts that are specific to the details of the Hamiltonian. As an example, the code here contains a module for application to the *sd*-shell with a shell-model Hamiltonian containing one-body and two-body terms. There is a long-term motivation for this application as well. The *sd*-shell could be a good testing ground for the extensions of SCMF such as the GCM and approximations derived from GCM. Since one has a Hamiltonian for the *sd*-shell that describes the structure very well, one could test the approximations to introduce correlations, such as projection, the random-phase approximation, etc and compare them with the exact results from the Shell Model. Preliminary results along this line are discussed in [11, 12]. As a first step in this program, one needs a robust SCMF code that treats shell-model Hamiltonians. Extensions to other shell model configuration spaces are straightforward and only limited by the availability of computational resources.

The code described here is more general than earlier published codes in that it can treat even or odd systems equally well. The formalism for the extension to odd systems and to a statistical density matrix will be presented elsewhere [13]. We also mention that the present code (with a different Hamiltonian module) has already been applied to investigate neutron-proton pairing in heavy nuclei[14].

II. SUMMARY OF THE GRADIENT METHOD

As emphasized above, he fundamental numerical problem to be addressed is the minimization of the mean value one- plus two-body Hamiltonian under the set of Bogoliubov transformations in a finite-dimensional Fock space. We remind the reader of the most essential equations, using the notation of Ring and Schuck [1]. The basic variables are the U and V matrices defining the Bogoliubov transformation. However, these are not the independent variables of the problem due to the restriction that the transformation is canonical. The main physical variables are the one-body matrices for the density ρ and the anomalous density κ, given by

$$\rho = V^* V^t; \quad \kappa = V^* U^t. \tag{1}$$

The Hamiltonian may be defined in the Fock-space representation as

$$\hat{H} = \sum_{12} \varepsilon_{12} c_1^\dagger c_2 + \frac{1}{4} \sum_{1234} v_{1234} c_1^\dagger c_2^\dagger c_4 c_3. \tag{2}$$

The expectation value of the Hamiltonian under a Bogoliubov transformation of the vacuum is given by

$$H^{00} \equiv \langle \hat{H} \rangle = \mathrm{Tr}(\varepsilon\rho + \tfrac{1}{2}\Gamma\rho - \tfrac{1}{2}\Delta\kappa^*). \tag{3}$$

in terms of the fields for the ordinary potential Γ and the pairing potential Δ. These are defined as

$$\Gamma_{12} = \sum_{34} v_{1423}\rho_{34}; \quad \Delta_{12} = \tfrac{1}{2}\sum_{34} v_{1234}\kappa_{34}. \tag{4}$$

The gradient method makes extensive use of the quasiparticle representation for operators related to the ordinary and anomalous densities. For a single-particle operator $\hat{F} = \sum_{ij} F_{ij} c_i^\dagger c_j$ we write

$$\sum_{ij} F_{ij} c_i^\dagger c_j \equiv c^\dagger F c = F^{00} + \beta^\dagger F^{11} \beta^\dagger + \tfrac{1}{2}\left(\beta F^{02}\beta + \beta^\dagger F^{20}\beta^\dagger\right). \tag{5}$$

where $\beta, \beta^\dagger$ are quasiparticle annihilation and creation operators. The gradient of the mean value of the operator F is given by the variation of this quantity with respect to the independent variables defining the Bogoliubov transformation. It is constructed from the skew-symmetric matrix F^{20}, which for a normal one-body operator is given by

$$F^{20} = U^\dagger F V^* - V^\dagger F^t U^*. \tag{6}$$

The corresponding representation for an operator $\hat{G}$ of the anomalous density is

$$\tfrac{1}{2}(c^\dagger G c^\dagger - c G^* c) = G^{00} + \beta^\dagger G^{11}\beta + \tfrac{1}{2}(\beta^\dagger G^{20}\beta^\dagger + \beta G^{02}\beta) \tag{7}$$

The skew-symmetric matrix G^{20} is given by

$$G^{20} = U^\dagger G U^* - V^\dagger G^* V^*. \tag{8}$$

Two operators that are particularly useful to characterize the HFB states are the axial quadrupole operator Q_Q and the number fluctuation operator ΔN^2. We define Q_Q as

$$Q_Q = 2z^2 - x^2 - y^2; \tag{9}$$

its expectation value distinguishes spherical and deformed minima. The number fluctuation is an indicator of the strength of pairing condensates and is zero in the absence of a condensate. It depends on the two-body operator $\hat{N}^2$, but like the Hamiltonian can be expressed in terms of one-body densities. We define it as

$$\Delta N^2 \equiv \langle \hat{N}^2 \rangle - \langle \hat{N} \rangle^2 = \frac{1}{2}\mathrm{Tr}\left(N^{20}N^{02}\right) = 2\mathrm{Tr}\left(\rho(1-\rho)\right) = -2\mathrm{Tr}\left(\kappa^*\kappa\right). \tag{10}$$

The full expansion of the Hamiltonian in the quasiparticle basis is given in Eqs. (E.20-E.25) of [1]. Here we will mainly need H^{20}, given by

$$H^{20} = h^{20} + \Delta^{20} = U^\dagger h V^* - V^\dagger h^t U^* - V^\dagger \Delta^* V^* + U^\dagger \Delta U^*. \tag{11}$$

where $h = \epsilon + \Gamma$. Starting from any HFB configuration U, V one can construct a new configuration U', V' by the generalized Thouless transformation. The transformation is defined by a complex skew-symmetric matrix Z having the same dimensions as U, V. All the elements z_{ij} with $i > j$ are independent. One often assumes that the transformation preserves one or more symmetries such as parity or axial rotational symmetry. Then the U, V matrices are block diagonal and Z has the same block structure. The transformation is given by

$$\begin{aligned} U' &= (U + V^*Z^*)(1 - ZZ^*)^{-1/2} = U + V^*Z^* + \mathcal{O}(Z^2) \\ V' &= (V + U^*Z^*)(1 - ZZ^*)^{-1/2} = V + U^*Z^* + \mathcal{O}(Z^2). \end{aligned} \tag{12}$$

The last factor, $(1 - ZZ^*)^{-1/2}$, ensures that the transformed set U', V' satisfies the required unitarity conditions for the Bogoliubov transformation. It can be efficiently computed using the Cholesky decomposition [9]. We now ask how the expectation value of some bilinear operator $\hat{Q}$ changes when the Thouless transformation is applied. The result is very simple, to linear order in Z:

$$Q^{00}_{new} = Q^{00} - \frac{1}{2}(\mathrm{Tr}(Q^{20}Z^*) + \mathrm{h.c.}) + \mathcal{O}(Z^2). \tag{13}$$

The same formula applies to the Hamiltonian as well,

$$H^{00}_{new} = H^{00} - \frac{1}{2}(\mathrm{Tr}(H^{20}Z^*) + \mathrm{h.c.}) + \mathcal{O}(Z^2). \tag{14}$$

From these formulas it is apparent that the derivative of the expectation value with respect

to the variables z^*_{ij} in Z^* is[1]

$$\frac{\partial}{\partial z^*_{ij}} Q^{00} = Q^{20}_{ij}. \tag{15}$$

With a formula for the gradient of the quantity to be minimized, we have many numerical tools at our disposal to carry out the minimization.

It is quite straightforward to introduce constraining fields in the minimization process. As seen in Eq. (13) the transformation Z will not change the expectation value of $\hat{Q}$ to linear order provided $\mathrm{Tr}(Q^{20}Z^*) + \mathrm{h.c.} = 0$. Thus, one can change the configuration without affecting the constraint (to linear order) by projecting Z to Z_c as $Z_c = Z - \lambda Q^{20}$ with $\lambda = \frac{1}{2}(\mathrm{Tr}(Q^{20}Z^*) + \mathrm{h.c.})/\mathrm{Tr}(Q^{20}Q^{20\,*})$. With multiple constraints, the projection has the form

$$Z_c = Z - \sum_\alpha \lambda_\alpha Q^{20}_\alpha. \tag{16}$$

The parameters λ_α are determined by solving the system of linear equations,

$$\sum_\alpha M_{\alpha\beta}\lambda_\alpha = \frac{1}{2}(\mathrm{Tr}(Q^{20}_\beta Z^*) + \mathrm{h.c.}) \tag{17}$$

where $M_{\alpha\beta} = \mathrm{Tr}(Q^{20}_\alpha Q^{20\,*}_\beta)$. Since we want to minimize the energy, an obvious choice for the unprojected Z is the gradient of the Hamiltonian H^{20}. In this case the constraining parameters λ_α are identical to the Lagrange multipliers in the usual HFB equations. We will use the notation H_c for the constrained Hamiltonian

$$H_c = H - \sum_\alpha \lambda_\alpha Q_\alpha. \tag{18}$$

A. Numerical aspects of the minimization

The most obvious way to apply the gradient method is to take the direction for the change from Eq. (16,17), and take the length of the step as an adjustable numerical parameter. We will call this the *fixed gradient* (FG) method. It is implemented in the program as

$$Z_\eta = \eta H^{20}_c. \tag{19}$$

Typically the starting U, V configuration will not satisfy the constraints, and the Z transformations must also bring the expectation values of the operators to their target values q_α.

[1] The derivative is taken with respect to the variables in the skew-symmetric Z^*, ie. $z^*_{ji} = -z^*_{ij}$ and z_{ij}, z^*_{ij} are treated as independent variables.

The error vector δq_α to be reduced to zero is given by

$$\delta q_\alpha = Q^{00}_\alpha - q_\alpha. \tag{20}$$

We apply Eq. (13) to first order to obtain the desired transformation $Z_{\delta q}$,

$$Z_{\delta q} = -\sum_{\alpha\beta} M^{-1}_{\alpha\beta} \delta q_\alpha Q^{20}_\beta. \tag{21}$$

With these elements in hand, a new configuration is computed using the transformation

$$Z = Z_c + Z_{\delta q}. \tag{22}$$

This process is continued until some criterion for convergence is achieved. We shall measure the convergence by the norm of the gradient $|H^{20}_c|$. This is calculated as

$$|H^{20}_c| = \left(\mathrm{Tr}[H^{20}_c (H^{20}_c)^\dagger]\right)^{1/2}. \tag{23}$$

An example using this method as given is shown in Fig. 1. The parameter η is fixed to some value and the iterations are carried out until convergence or some upper limit is reached. The required number of iterations varies roughly inversely with η, up to some point where the process is unable to find a minimum in a reasonable number of iterations.

There are a number of ways to speed up the iteration process. If the constraints are satisfied, the parameter η can be increased considerably. Fig. 2 shows the change in H^{00}_c from one iteration cycle as a function of η using Z_c to update. For small values of η, the change in constrained energy is given by the Taylor expansion Eq. (14), $\Delta H^{00}_c \approx -\eta Tr\,(H^{00*}_c H^{00}_c)$. This function is shown as the straight line in the Figure. The actual change is shown by the black circles. One sees that η could be doubled or tripled from the maximum value permitted in Fig. 1. However, the constraints and other aspects of the new U, V become degraded so that such steps are not permissible for many iterations [2]. Still, one can take advantage of the possible improvement by choosing η at each iteration taking account of the relevant information from the previous iteration. This can be extracted from the ratio

$$r = \frac{\Delta H^{00}_c}{\eta \mathrm{Tr}\,(H^{00*}_c H^{00}_c)} \tag{24}$$

which is close to one for too-small η values and close to $\frac{1}{2}$ at the value corresponding to the steepest-descent minimum. We call such methods *variable gradient*. We note that updates with $Z_{\delta q}$ alone are relatively quick because there is no need to evaluation matrix elements

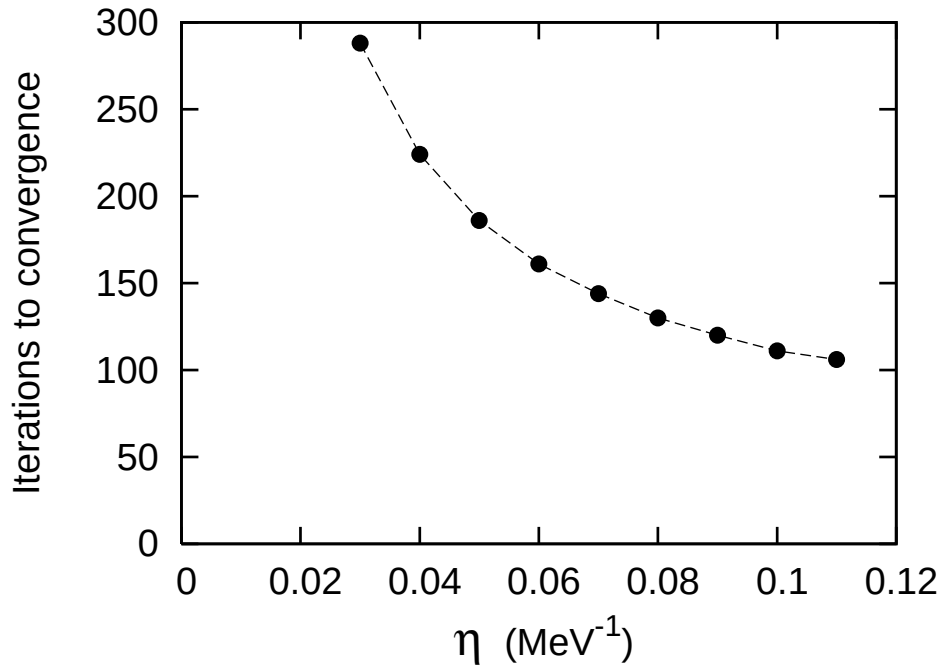

FIG. 1: Number of iterations required for convergence using Eq. (19) and fixed η. At the point $\eta = 0.12$ MeV^{-1} and beyond, the iteration process is unstable. The converged solutions and their energies are the same for all values of η shown in the plot. All values producing converged solutions The system is ^{24}Mg with three constraints, N, Z, and $< Q_Q >= 10\ \hbar/m\omega_0$. The convergence criterion is $|H_c^{20}| < 1.0 \times 10^{-2}$ MeV. See Section VI B for further details.

of the Hamiltonian. These considerations are implemented in the code of Ref. [10] by interspersing cycles of iteration by $Z_{\delta q}$ alone among the cycles with updates by Eq. (22).

Another way to improve the efficiency of the iteration process is to divide the elements of H_c^{20} by preconditioning factors p_{ij},

$$(Z_c)_{ij} = \eta \frac{(H_c^{20})_{ij}}{p_{ij}}. \tag{25}$$

The choice of the preconditioner is motivated by Newton's method to find zeros of a function (here H_c^{20}) based on knowledge of its derivative. This could be accessible from the second-order term in Eq. (14), but unfortunately it cannot be easily computed as it involves the HFB stability matrix. However a reasonable approximation to it can be obtained from H_c^{11}, the one-quasiparticle Hamiltonian that, when in diagonal form, is the dominant component of the diagonal of the stability matrix. One first transforms U, V to a basis that diagonalizes H_c^{11}. Call the eigenvalues of the matrix E_i and the transformation to diagonalize it C. The U, V are transformed to U', V' in the diagonal quasiparticle basis

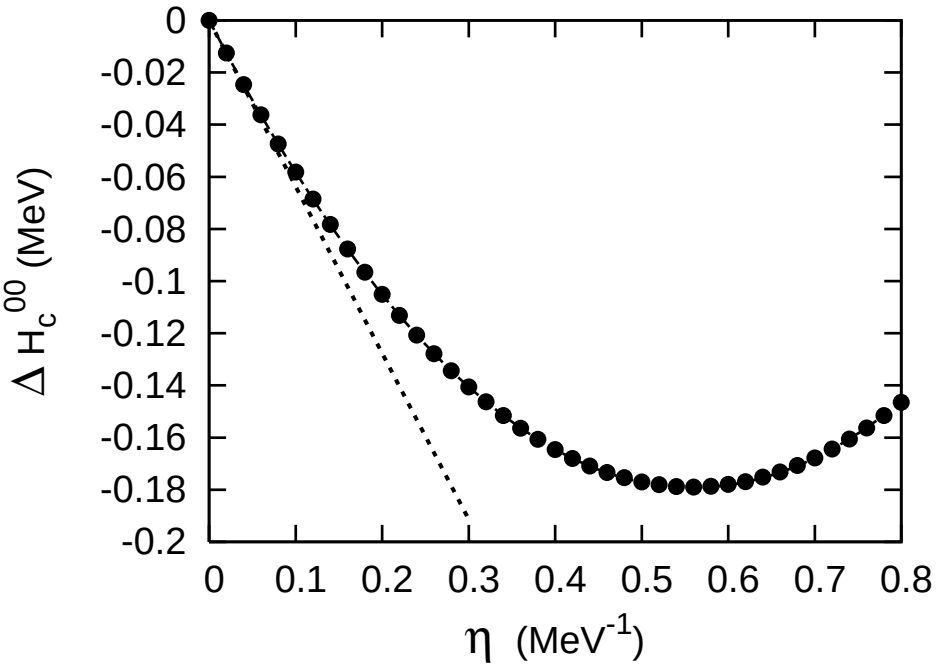

FIG. 2: Single-step energy change as a function of η in Eq. (19). The configuration that was updated is the 10th iteration step of the system in Fig. 1.

by

$$U' = UC; \quad V' = V'C \tag{26}$$

In the new basis the preconditioner is given by

$$p_{ij} = \max(E_i + E_j, E_{min}) \tag{27}$$

where E_{min} is a numerical parameter of the order of 1-2 MeV. The main effect of the preconditioner is to damp away those components of the gradient with high curvatures (i.e. second derivatives) which correspond to two-quasiparticle excitations with large excitation energies. This is very important for Hamiltonians that have a large range of single-particle energies, such as the ones derived from commonly used nuclear energy density functionals such as Skyrme and Gogny.

In Table I we show the number of iterations required to reach convergence for a case calculated in Table II, to be described below. We see that there is a gain of more than a factor of 3 between the naive steepest descent and the preconditioned gradient with a variable η. Similar ideas have been used in a HF context in [2, 15] with similar speedups.

Method	η	η_{min}	η_{max}	I_{conv}
fixed gradient	0.10 MeV^{-1}			140
variable gradient		0.08 MeV^{-1}	0.3 MeV^{-1}	65
fixed pr.	0.7			72
variable pr.		0.7	2.0	34

TABLE I: Number of iterations to convergence I_{conv} with various treatments of the update. Eq. (19) with fixed and variable gradients is used for the top two lines and the preconditioned gradients Eq. (25) are used for the lower two lines. The system is ^{21}Ne as calculated in the top first entry in Table II.

B. The starting configuration

It is important to understand the role of the starting configuration in the gradient search. It is crucial in determining the number parity, as will be discussed in the next section. But also it is important for other aspects of the iterative process. The energy H^{00} is a quadratic function of symmetry-breaking densities because the products of densities in the functional must respect the symmetries of the Hamiltonian. If these components are zero in the initial configuration, the energy is stationary at that point and there is no gradient to generate nonzero field values. The typical cases are quadrupole deformation in the ordinary density and any form of anomalous densities. Fortunately, it is very easy to avoid unwanted symmetries in the starting U, V. To insure that the solution allows for quadrupole deformation, one may impose a nonzero quadrupole constraint and then relax it. In fact, this is often carried out by first calculating the energy curve as a function of deformation, and then searching for the ground state using the lowest energy configurations to start the unconstrained minimization. This avoids the very slow convergence when the energy curve is nearly flat.

Other kinds of unwanted symmetries are harder to anticipate. In particular, the many channels of pairing allowing the full spin and isospin degrees of freedom can only be accessed from a starting configuration that has a nonzero condensate. A powerful way to deal with all of these cases is to apply a random Z transformation to the starting configurations before using them in the gradient search. We will illustrate both of these methods in the examples below, denoting the randomized starting configurations by U_r, V_r.

III. ODD-A NUCLEI

As discussed by Ring and Schuck[1], each U, V set can be characterized by its number parity, either even or odd. This means that when the wave function is constructed and states of definite particle number are projected out, the nonzero components will have either all even or all odd particle number. Another important fact is that the generalized Thouless transformation does not change the number parity of the Bogoliubov transformation. Thus, if we start from a U, V set of odd number parity, the final converged configuration will only have components of odd nucleon number.

In fact, in the matrix-diagonalization method of solving the HFB equations, the higher energy of the odd-A configurations requires some modification to the Hamiltonian or to the iteration process. A common solution is to add additional constraining fields so the that odd-A system has lower energy[16, 17]. Typically the external field to be added breaks time reversal symmetry in some way. But then one can no longer assert that a true minimum has been found, because the extra constraints can affect the configuration. The gradient method does not have this shortcoming. If the space of odd-number parity Bogoliubov transformations is adequately sampled, it will find the global minimum of the odd-A configurations. Moreover, with the gradient method one does not need to modify the computer code to treat odd-A systems. Only the initial U, V set is different for the two cases.

We note the H_c^{11} has negative quasiparticle eigenenergies in the odd number-parity space, assuming that the true minimum of the HFB functional is an even number-parity configuration.

IV. IMPOSED SYMMETRIES

The U, V matrices have a dimension of the size of the Fock space of nucleon orbitals and in principle can be dense matrices. However, one often imposes symmetries on the wave function by assuming that the U, V have a block structure with all elements zero outside the blocks. For example, most codes assume separate blocks for neutrons and protons. This is well-justified when there is a significant difference in neutron and proton numbers but in general it is better to allow them to mix. Other quantum numbers that are commonly imposed on the orbital wave functions are parity and axial symmetry. There are only a

few exceptional nuclei that have HFB ground states breaking these symmetries. For the parity, there are the Ra nuclei and Th nuclei. Concerning axial symmetry, a global study of even-even nuclei with the Gogny functional [18] found only three cases of nonaxial HFB minima among 1712 nuclei.

The number of orthogonal minima that can be easily calculated in the gradient method depends on the assumed block structure. In the even number-parity space there is just one global minimum. But in the odd number-parity space the number parity of each block is conserved in the iteration process, so there will be one state for each block. For example, states of different K-quantum number may be calculated by imposing a block structure that imposes axial symmetry. Thus for odd-A nuclei, the quasiparticle can be in any of the K-blocks, giving a spectrum of states with K specified by the block.

V. THE CODE HFB_SHELL

The code `hfb_shell` presented in this paper is described in more detail in the Appendix. The main point we want emphasize about the code is that it is organized in modules that separate out the functions that are independent of the Hamiltonian from those that are specific to it. Also, the block structure is specified only by the code input, and can easily be changed. The examples we show are for the *sd*-shell using the USDB Hamiltonian [19]. Since that Hamiltonian is specified by the fitted numerical values of the 3 single-particle energies and the 63 JT-coupled two-particle interaction energies, it does not have any symmetries beyond those demanded by the physics. In particular, the HFB fields obtained with it should provide a realistic description of aspects such as the time-odd fields, that are difficult to assess with the commonly used energy functionals such as those in the Skyrme family.

A. Application to the *sd*-shell

The *sd* shell-model space has a dimension of 24 and the principal matrices $U, V, Z, ...$ have the same dimension. In the application presented here, we assume axial symmetry which splits the matrices in blocks of dimension 12, 8 and 4 for m-quantum numbers $\pm\frac{1}{2}$, $\pm\frac{3}{2}$, and $\pm\frac{5}{2}$ respectively. Neutron and proton orbitals are in the same blocks, so the basis is sufficiently general to exhibit neutron-proton pairing, if that is energetically favorable. We

also assume that the matrices are real.

We often start with a U, V configuration of canonical form, namely U diagonal, $U_{ij} = u\delta_{ij}$. The nonzero entries of the V are all equal to $\pm v = \pm\sqrt{1-u^2}$, and are in positions corresponding to pairing in the neutron-neutron channel and the proton-proton channel. We arbitrarily take $u = 0.8$ and $v = 0.6$ for the starting configuration U_0, V_0. This may be modified in a number of ways before it is used as a starting configuration in the gradient minimization. When calculating a nucleus for which N or Z is zero or 12, it is more efficient to use U, V matrices that have those orbitals empty or completed filled in the starting configuration. This is carried out by changing u, v to zero or one for the appropriate orbitals. The particle number of that species is then fixed and is not constrained in the gradient search.

For odd-number parity configurations, the U, V is changed in the usual way by interchanging a column in the U matrix with the corresponding column in V. The space that will be searched in the gradient method then depends on the block where the interchange was made. In principle it does not depend on which column of the block was changed. However, there is some subtlety is making use of this independence which will be discussed below.

In principle one could also start from the U, V configuration of the vacuum: $U = 1, V = 0$. We have tried this and found, as might be expected, that the proportion of false minima is larger than is obtained with U_0, V_0.

VI. THREE EXAMPLES

In this section we will describe the HFB calculations for three nuclei, ^{32}Mg, ^{24}Mg, and ^{21}Ne. The first one is typical of a spherical nucleus that exhibits identical-particle pairing. The second is a well-deformed nucleus. The third illustrates the method for an odd-A system.

For calculating matrix elements of the quadrupole operator Q_Q, we will treat the single-particle wave functions as harmonic oscillator functions of frequency ω_0, and report the quadrupole moments in units of $\hbar/m\omega_0$.

A. ^{32}Mg

The nucleus ^{32}Mg ($(N, Z) = (12, 4)$ in the *sd*-shell) behaves as expected of a semimagic nucleus in HFB. Please note that we do not include in our configuration space the $f_{7/2}$ intruder shell required to explain the deformation properties of this nucleus [20, 21]. We calculate the HFB ground state in two ways, illustrating the role of the starting configuration. The first is to use a randomized U_r, V_r configuration and constraining the particle numbers to the above values. Another way is to start with a prolate configuration similar to U_0, V_0 for the protons and with all the neutron orbitals filled. In that case, only the proton number is constrained. Both iteration sets converge to the same minimum, a spherical configuration having a strong proton pairing condensate. The output characteristics are $E_{HFB} = -135.641$ MeV, $Q_Q^{00} = 0.00$ and $\Delta Z^2 = 2.93$. The zero value for Q_Q^{00} shows that the configuration is spherical, and the nonzero value for ΔZ^2 shows that protons are in a condensate. Next we calculate the condensation energy, defined as the difference between E_{HFB} and the Hartree-Fock minimum E_{HF}. The easiest way to find the HF minimum is to repeat the calculation with an additional constraint that forces the condensate to zero. This is done by adding a G-type operator that is sensitive to the presence of a condensate. Carrying this out, we find a minimum at $E_{HF} = -134.460$ MeV and $Q_Q^{00} = 5.08$. The extracted correlation energy is $E_{HF} - E_{HFB} = 1.18$ MeV, which is much smaller than what one would obtain with schematic Hamiltonians fitted to pairing gap. It is also interesting to extract the quasiparticle energies, since they provide the BCS measure of the odd-even mass differences. These are obtained by diagonalizing H_c^{11}. The results for the HFB ground state range from 1.5 to 9 MeV, with the lowest giving the BCS estimate of the pairing gap.

B. ^{24}Mg

The next nucleus we consider, ^{24}Mg with $N = 4$ and $Z = 4$, is strongly deformed in the HFB ground state. We find that the converged minimum has a quadrupole moment $\langle Q_Q \rangle = 12.8$, close to the maximum allowed in the space. More surprisingly, the pairing condensate vanishes at the HFB convergence. We now make a set of constrained calculations to display the energy as a function of quadrupole moment. The starting configuration is generated by applying a random transformation to U_0, V_0. The gradient code carries out the

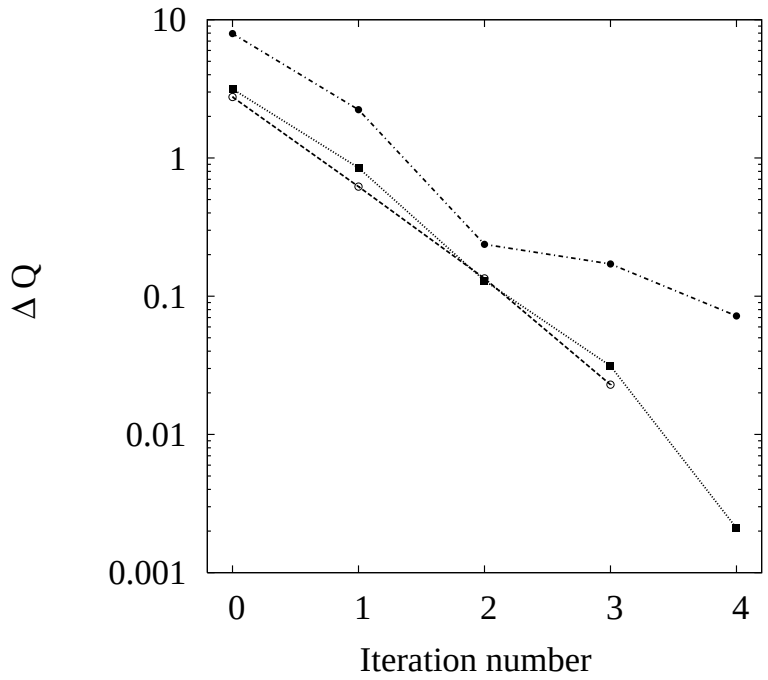

FIG. 3: Error in constrained quantities as a function of iteration number for the $\eta = 0.1$ run of the ^{24}Mg iterations in Fig. 1. Quantities constrained are: N, open circles; Z, filled squares; and Q_Q, filled circles.

iterations with the constraints $N = 4$, $Z = 4$, and the chosen value of Q. The convergence of the constraints to their target values is very rapid, using the update in Eq. (21). This is illustrated in Fig. 3, showing the deviation from the target values as a function of iteration number in one of the cases ($Q = 10$). On the other hand, the convergence to the minimum of the HFB energy can be slow, using a fixed-η update with Eq. (19). The calculations were carried out setting the convergence criterion $|H_c^{20}| < 0.01$ MeV. Fig. 4 shows the number of iterations required to reach convergence for the various deformations. They range from 40 to 250. In a number of cases, the iterations seem to be approaching convergence, but the system is actually in a long valley, and eventually a lower minimum is found. It may also happen that the gradient method finds a local minimum that is not the global one. This can often be recognized when carrying constrained calculations for a range of constraint values, as it gives rise to discontinuities in the energy curves. We show in Fig. 5 the energies as a function of deformation made by combining two runs starting from each side, and taking the lowest energy at each point. The global minimum is at a large prolate deformation as

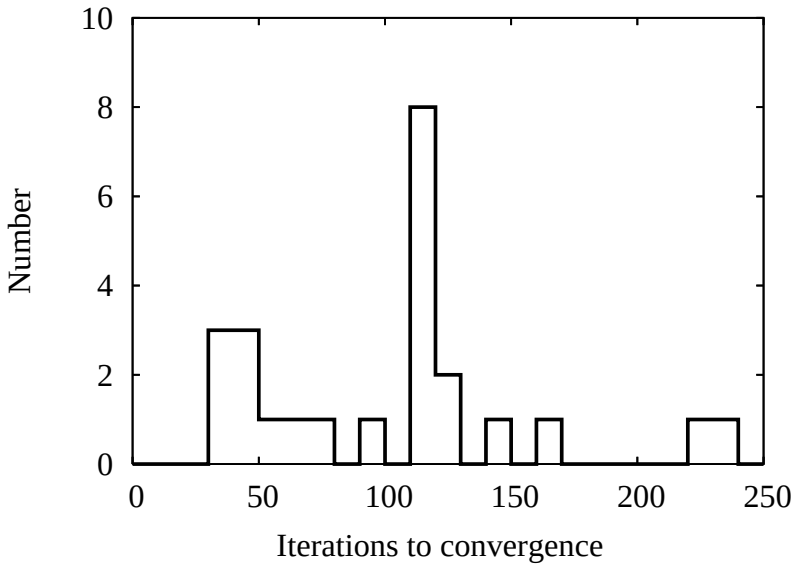

FIG. 4: Number of iterations required to convergence for the calculated configurations on the deformation energy curve Fig. 5.

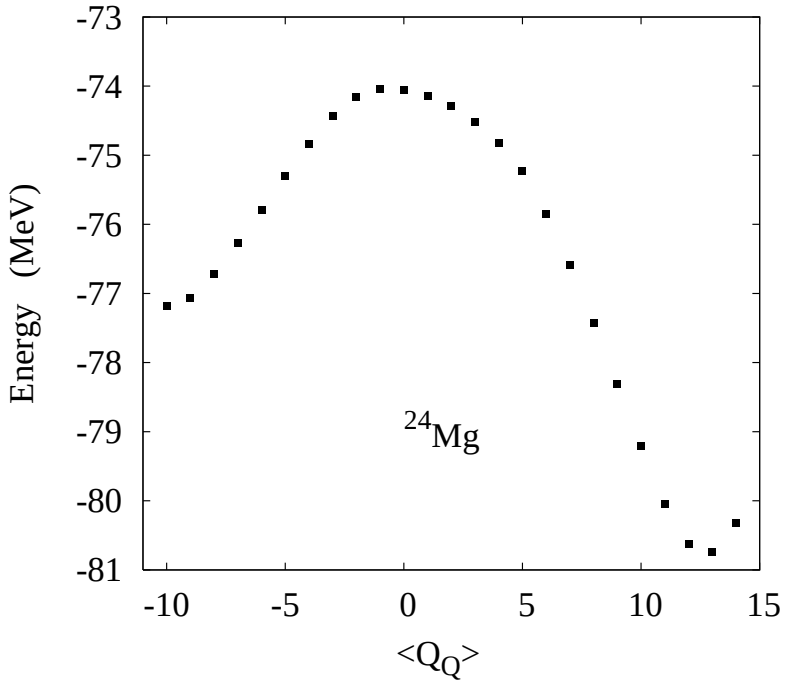

FIG. 5: HFB energies as a function of deformation, using the Q_Q quadrupole constraint. The nucleus is ^{24}Mg, $N = Z = 4$ in the *sd*-shell.

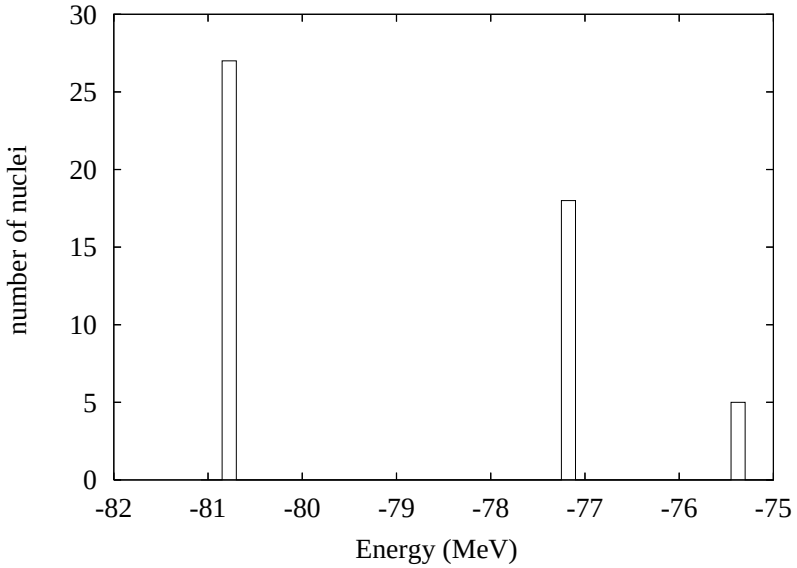

FIG. 6: Local minima for 50 runs of ^{24}Mg with different random starting configurations. Shown are the number of cases as a function of energy.

mentioned earlier. There is also a secondary minimum at a large oblate deformation. For all deformations, the ordinary neutron-neutron and proton-proton pairing condensates are small or vanish.

A global picture of the different minima can be obtained using randomized starting UV configurations. For this exercise, we have carried out the minimization from 50 different starting configurations, imposing only particle-number constraints on the ^{24}Mg iterations. The first configuration was generated from the vacuum state. Successive configurations were constructed by applying to the previous configuration a transformation Z whose independent elements are sampled from a Gaussian distribution with zero mean and a variance $\langle z_{ij}^2 \rangle^{1/2} = 2$. We find that all runs converged, and there were just three converged states. A histogram of the number of cases for each state is shown in Fig. 6. We see that both minima that appear on Fig. 5 are present, as well as a third local minimum at somewhat higher energy. The lowest energy, -80.76 MeV, is the most likely to be obtained from a random starting configuration. This gives one a high degree of confidence that the state is in fact the global minimum.

C. ^{21}Ne

The next nucleus we discuss, ^{21}Ne with $(N,Z)_{sd} = (3,2)$, illustrates how the gradient method makes use of the conserved number parity to find the minimum of odd-A systems. We start with the U_0, V_0 configuration, and convert it to an odd-number parity configuration by exchanging two columns in the $m = \pm\frac{1}{2}$ block. There are 6 possible columns with $m = +\frac{1}{2}$ that can be exchanged. The results for the converged energies are shown in the top row of Table II. All of the neutron exchanges give the same final energy, -40.837 MeV. However, the energy is different for proton exchanges. The reason is that the starting configurations do not mix neutrons and protons, and for reasons discussed earlier the corresponding gradients are zero. This unwanted symmetry can be broken by making a random transformation of the initial configuration. The results are shown in the second row. Now all the energies are equal, showing that the minimum can be accessed from any column exchange. Interestingly, the energy is lower than in the previous set of minimizations. This shows that there is a significant neutron-proton mixing in the condensate for ^{21}Ne.

U,V	$d^n_{5/2,1/2}$	$d^n_{3/2,1/2}$	$s^n_{1/2,1/2}$	$d^p_{5/2,1/2}$	$d^p_{3/2,1/2}$	$s^p_{1/2,1/2}$
U_0, V_0	-40.837	-40.837	-40.837	-40.215	-40.176	-40.176
U_r, V_r	-41.715	-41.715	-41.715	-41.715	-41.715	-41.715

TABLE II: HFB energies of ^{21}Ne, with different starting configurations. For the top row, the starting configuration is U_0, V_0 with the indicated column in the $m = \pm\frac{1}{2}$ block interchanged. The second row starts from a randomized configuration U_r, V_r as discussed in Sect. V A.

Acknowledgments

The authors thank A. Gezerlis and P. Ring for discussions, T. Lesinski and J. Dobaczewski for comments on the manuscript, and M. Forbes for comments on the code. This work (GFB) was supported in part by the U.S. Department of Energy under Grant DE-FG02-00ER41132, and by the National Science Foundation under Grant PHY-0835543. The work of LMR was supported by MICINN (Spain) under grants Nos. FPA2009-08958, and FIS2009-07277, as well as by Consolider-Ingenio 2010 Programs CPAN CSD2007-00042 and MULTIDARK

CSD2009-00064.

---

[1] P. Ring and P. Schuck, *The nuclear many-body problem*, (Springer, 1980).

[2] P.-G. Reinhard and R.Y. Cusson, Nucl. Phys. **A378** 418 (1982).

[3] K.T.R. Davies, H. Flocard, S. Krieger, and M.S. Weiss, Nucl. Phys. **A342** 111 (1980).

[4] P. Bonche, H. Flocard, and P.-H. Heenen, Comput. Phys. Commun. **171** 49 (2005).

[5] J. Dobaczewski, and P. Olbratowski, Comput. Phys. Commun. **167** 214 (2005).

[6] K. Bennaceur and J. Dobaczewski, Comp. Phys. Commun. **168** 96 (2005)

[7] W. Pöschl, D. Vretenar, A. Rummel, and P. Ring, Comput. Phys. Commun. 101 75 (1997).

[8] M. Stoitsov, et al., Comput. Phys. Commun. **167** 43 (2005).

[9] J.L. Egido, J. Lessing, V. Martin, and L.M. Robledo Nucl. Phys. **A594** 70 (1995)

[10] M. Warda, J.L. Egido, L.M. Robledo, and K. Pomorski, Phys. Rev. C **66** 014310 (2002).

[11] I. Maqbool, J.A. Seikh, P.A. Ganai, and P.Ring, J. Phys. G: Nucl. Part. Phys. **38** 045101 (2011).

[12] R. Rodríguez-Guzmán, Y. Alhassid, and G.F. Bertsch, Phys. Rev C**77**, 064308 (2008)

[13] L.M. Robledo and G.F. Bertsch, in preparation.

[14] A. Gezerlis, G.F. Bertsch, and L. Luo, arXiv:1103.5793 (2011).

[15] A.S. Umar, et al. Phys. Rev. **C32** 172 (1985).

[16] G.F. Bertsch, J. Dobaczewski, W. Nazarewicz, and J. Pei, Phys. Rev. A **79** 043662 (2009).

[17] B. Banerjee, P. Ring, and H.J. Mang, Nucl. Phys. A **215** 266 (1973).

[18] J.-P. Delaroche, et al., Phys. Rev. C **81** 014303 (2010).

[19] B.A. Brown and W.A. Richter, Phys. Rev. C **74** 034315 (2006).

[20] T. Motobayashi, et al., Phys. Lett. **B346** 9 (1995).

[21] R.Rodríguez-Guzmán, J.L. Egido, and L.M. Robledo Nucl. Phys. **A709** 201 (2002).

[22] K. J. Millman and M. Aivazis, Comp. Sci. Eng. **13** 9 (2011)

Appendix: explanation of the code

The code `hfb_shell` that accompanies this article implements the gradient method discussed in the text[2] The code is written in Python and requires the Python numerical library `numpy` to run (see [22] and accompanying papers for a description of Python in a scientific environment). The main program is contained in `hfb.py`. It first carries out the initialization using information from the primary input data file that in turn contains links to other needed data files. There are three of these, one for the Hamiltonian parameters, one for the correspondence between orbitals and rows of the U, V matrices include the assumed block structure, and one for the input U, V configuration. The input data format is explained in the `readme.txt` of the code distribution.

Following initialization, program enters the iteration loop, calling the various functions used to carry out the iteration. The loop terminates when either a maximum number of iterations `itmax` is reached or the convergence parameter $|H_c^{20}|$ go below a set value `converge`.

The function calls that are specific to the *sd*-shell application are collected in the module `sd_specific.py`. The tasks carried out by these functions include:

- initialization of matrix sizes and block structures
- setting up the matrices representing single-particle operators in the shell-model basis.
- calculation of the fields Γ, Δ from the densities ρ, κ. This function makes use of a table of interaction matrix elements v_{ijkl} that are read in from a file. The present distribution of the code only provides the Hamiltonian data for the USDB interaction [19].

The functions that are generic to the gradient method are collected in the module `hfb_utilities.py`. Many of these functions are defined by equations in the text; the correspondence is given in Table III.

The output of `hfb.py` reports the expectation values of the Hamiltonian and the single-particle operators N, Z and Q_Q at each iteration step, together with the convergence parameter $|H_c^{20}|$. After the final iteration, the values are reported for the expectation values

[2] See the EPAPS archive.

Function call	Equation in text
`rho_kappa`	(1)
`F20`	(6)
`G20`	(8)
`H20`	(11)
`H00`	(3)
`Ztransform`	(12)

TABLE III: Python functions in `hfb_utilities.py` corresponding to equations in the text.

of constraining parameters λ_α and the number fluctuations $\Delta N^2, \Delta Z^2$. The final U, V configuration is written to the file `uv.out`. Thus additional iterations can be performed simply by specifying `uv.out` as the new input file.

In addition, there is a set of functions collected in the module `hfb_tools.py`. These are useful for making input U, V configurations and for analyzing the output U, V configuration, but are not needed to run `hfb.py`. For example, a randomizing transformation can be applied to a U, V configuration by the function `randomize`. Another useful function is `canonical`, used to extract the eigenvalues of the ρ operator needed for the canonical representation.